

ORIGINAL RESEARCH

Novel Receptor for Advanced Glycation End Products-Blocking Antibody to Treat Diabetic Peripheral Artery Disease

Lynne L. Johnson, MD ; Jordan Johnson , MS; Rebecca Ober , DVM; April Holland, CNMT; Geping Zhang, MD; Marina Backer , PhD; Joseph Backer , PhD; Ziad Ali , MD, PhD; Yared Tekabe , PhD

BACKGROUND: Expression of receptor for advanced glycation end products (RAGE) plays an important role in diabetic peripheral artery disease. We proposed to show that treatment with an antibody blocking RAGE would improve hind limb perfusion and muscle viability in diabetic pig with femoral artery (FA) ligation.

METHODS AND RESULTS: Purpose-bred diabetic Yucatan minipigs with average fasting blood sugar of 357 mg/dL on insulin to maintain a glucose range of 300 to 500 mg/dL were treated with either a humanized monoclonal anti-RAGE antibody (CR-3) or nonimmune IgG. All pigs underwent intravascular occlusion of the anterior FA. Animals underwent (^{201}Tl) single-photon emission computed tomography/x-ray computed tomography imaging on days 1 and 28 after FA occlusion, angiogenesis imaging with [$^{99\text{m}}\text{Tc}$]dodecane tetra-acetic acid-polyethylene glycol-single chain vascular endothelial growth factor (scVEGF), muscle biopsies on day 7, and contrast angiogram day 28. Results showed greater increases in perfusion to the gastrocnemius from day 1 to day 28 in CR-3 compared with IgG treated pigs ($P=0.0024$), greater uptake of [$^{99\text{m}}\text{Tc}$]dodecane tetra-acetic acid-polyethylene glycol-scVEGF (scV/Tc) in the proximal gastrocnemius at day 7, confirmed by tissue staining for capillaries and vascular endothelial growth factor A, and less muscle loss and fibrosis at day 28. Contrast angiograms showed better reconstitution of the distal FA from collaterals in the CR-3 versus IgG treated diabetic pigs ($P=0.01$). The gastrocnemius on nonoccluded limb at necropsy had higher ^{201}Tl uptake (percentage injected dose per gram) and reduced RAGE staining in arterioles in CR-3 treated compared with IgG treated animals ($P=0.04$).

CONCLUSIONS: A novel RAGE-blocking antibody improved hind limb perfusion and angiogenesis in diabetic pigs with FA occlusion. Contributing factors are increased collaterals and reduced vascular RAGE expression. CR-3 shows promise for clinical treatment in diabetic peripheral artery disease.

Key Words: antibodies ■ diabetes mellitus ■ peripheral artery disease

Peripheral artery disease (PAD) is a worldwide medical problem. Using an ankle-brachial index <0.90 as cutoff, a global epidemiological study found in high-income countries an increase in prevalence from 5% at the age of 45 to 49 years to 18% by the age of 85 to 89 years.¹ In the CCHS (Copenhagen City Heart Study), proportion of patients with symptomatic claudication increased from 0% among those aged 35 to 44 years to 31% among those aged 65 to 74 years.² Symptomatic PAD is twice as common

among those with diabetes mellitus, and although insulin resistance in type 2 diabetes mellitus is a contributing factor, the level of blood sugar has the most important association for developing symptomatic PAD.² For a 1% increase in hemoglobin A1c, the incidence of symptomatic PAD increases by 26%.² The presence of PAD is high among those with diabetic foot ulcers and a major contributor to poor wound healing and greater morbidity, mortality, and amputation.³⁻⁵ Current 2016 American Heart Association/

Correspondence to: Lynne L. Johnson, MD, Columbia University Medical Center, 622 W 168th St, PH 10-203, New York, NY 10032. E-mail: lj2129@cumc.columbia.edu

For Sources of Funding and Disclosures, see page 11.

© 2020 The Authors. Published on behalf of the American Heart Association, Inc., by Wiley. This is an open access article under the terms of the Creative Commons Attribution-NonCommercial-NoDerivs License, which permits use and distribution in any medium, provided the original work is properly cited, the use is non-commercial and no modifications or adaptations are made.

JAHA is available at: www.ahajournals.org/journal/jaha

CLINICAL PERSPECTIVE

What Is New?

- In this report, we are the first to show in a large animal model of diabetes mellitus and anterior femoral artery occlusion that treatment with a humanized antibody blocking receptor for advanced glycation end products compared with nonimmune IgG improves hind limb perfusion and muscle viability by suppressing detrimental effects of receptor for advanced glycation end products on hind limb ischemia.
- Our findings include the following: improved perfusion in both the ischemic limb with greater collateral formation and in the nonischemic hind limb attributed to reduced vascular disease; and removal of the suppressive effect of receptor for advanced glycation end products on the angiogenic response to hypoxia with capillary growth in the gastrocnemius muscle, supplied by the occluded artery and improved muscle viability.

What Are the Clinical Implications?

- These results suggest that treatment with a receptor for advanced glycation end products blocking antibody is a promising approach to treating diabetic peripheral artery disease.

Nonstandard Abbreviations and Acronyms

CR-3	anti-RAGE antibody
FA	femoral artery
FAL	femoral artery ligation
FAO	femoral artery occlusion
RAGE	receptor for advanced glycation end products

American College of Cardiology management guidelines for symptomatic diabetic PAD include control of risk factors, antiplatelet drugs, statins, and antihypertensives, including angiotensin-converting enzyme inhibitor/angiotensin II receptor blocker.⁶ The drug cilostazol has shown some clinical benefit.⁷ Despite these management and treatment strategies, many patients require revascularization. Intravascular interventional approaches have largely replaced surgical revascularization because of postoperative complications, including poor wound healing, in patients with diabetes mellitus.⁸ Arterial stenting has presented challenges because of length of lesions, bending of vessels with motion, and tendency for in-stent restenosis in diabetes mellitus.⁸ Developing

novel therapies to treat PAD represents an important unmet clinical need.

Receptor for advanced glycation end products (RAGE) is a 45-kDa transmembrane multiligand receptor of immunoglobulin superfamily that plays an important role in the cause and progression of PAD in diabetes mellitus.⁹ RAGE/ligand binding activates multiple pathways in the vascular wall, including generation of reactive oxygen species, increased vascular permeability, and release of cytokines and inflammation, thereby leading to diffuse atherogenesis and microvascular disease.^{9–15} The expression of RAGE increases as circulating ligands increase through a positive feedback cycle. In addition, RAGE suppresses the hypoxic response to release vascular endothelial growth factor (VEGF) and is a major contributor to failure of collateral growth in response to total vessel occlusion.^{16–19} Loss of angiogenesis and reduction in collateral formation in response to vascular occlusion lead to chronic hypoxia, muscle loss, and fibrosis.

Blocking RAGE expression to treat PAD represents a multipronged approach to block these pathways leading to diabetic vascular disease. We developed a monoclonal anti-RAGE antibody that binds a novel peptide sequence on the extracellular domain of the receptor, thereby preventing ligand binding. In diabetic mice with femoral artery ligation (FAL), treatment with anti-RAGE antibody improved angiogenesis at day 5 and hind limb blood flow at day 21 after FAL.²⁰ The mouse hind limb lacks the anatomical size and complexity of human disease. Our hypothesis was that we can detect a beneficial therapeutic effect of our anti-RAGE antibody versus placebo in a diabetic pig with hind limb anterior femoral artery occlusion (FAO), using multimodality single-photon emission computed tomography/x-ray computed tomography (SPECT/CT) imaging of perfusion and angiogenesis, angiography, and histology to evaluate outcomes.

METHODS

The data that support the findings of this study are available from the corresponding author on reasonable request.

Animals

All animal experiments were performed with the approval of the Institutional Animal Care and Use Committee of Columbia University. Purpose-bred diabetic Yucatan minipigs (castrated male, 27–30 kg) were obtained from Sinclair Laboratories (Auxvasse, MO). The Sinclair diabetic Yucatan minipigs have type 1 diabetes mellitus induced with alloxan and are sent to

investigators when diabetes mellitus is established and the blood sugar stabilized in range of 300 to 500 mg/dL on 7 to 8 units NPH Humulin N (range, 2–12 units). Only male pigs were used. Justification for using only male animals is based on the available model. Because of the technical effort required to create the model, the expense for each animal is high. To factor in effect of female hormones in addition to the effect of drug would require a large sample size and more complex study design, which was beyond the scope of the work proposed.

After arriving at Columbia University, we used an insulin dose range (Humulin-N) provided by Sinclair to maintain blood glucose in the desired range. We used the following sliding scale. Morning insulin dose was the following: for blood glucose >650 mg/dL, give 5 U of insulin; 301 to 650, give 4 U of insulin; 201 to 300, give 3 U of insulin; and 101 to 200, give 0 U of insulin. Afternoon insulin dose was the following: for blood glucose >500 mg/dL, give 7 U of insulin; 401 to 500, give 6 U of insulin; 301 to 400, give 5 U of insulin; 151 to 300, give 4 U of insulin; 51 to 150, give 2 U of insulin; and 20 to 50, give 1 U of insulin. Blood sugar was monitored twice daily with a handheld glucometer (Accu-check Aviva; Roche, Basel, Switzerland), and additional doses of regular insulin were given as needed. The veterinary staff weighed pigs weekly and observed them daily for signs of hyperglycemia or hypoglycemia. Blood samples were obtained for RAGE ligands from each pig on arrival before treatment and on the day of euthanasia.

Antibody

Each pig was injected IM with 1 mg/kg of either CR-3 or isotype-matched nonimmune IgG every 10 days over 4 weeks. The first dose was given after conditioning and 3 to 5 days before FAO.

Placement of Endovascular Occluder in Anterior Femoral Artery

Pigs were sedated, intubated, anesthetized, and maintained on isoflurane inhalant for the duration of the procedure. After sterile skin preparation, a cut down was

performed on the neck, the carotid artery was isolated, and catheters were advanced to the iliofemoral trunk using small injections of contrast to identify catheter location (OEC digital fluoroscope model 7900) (General Electric, Chicago, IL). An end hole catheter was advanced to the anterior femoral artery (FA) just distal to the takeoff of the circumflex branch where an Amplatzer Vascular Plug II, 8 mm (9-AVP2-008) (Abbott Laboratories, Abbott Park, IL), was deployed into the arterial lumen. The plug is oversized compared with the vessel diameter and designed for vascular closure, acting as a barrier and becoming endothelialized. After deployment of the occluder, a contrast angiogram was performed. The catheters were removed, the artery was repaired, and the neck wound was closed.

Radiotracer Injection and Hind Limb Perfusion Imaging

The protocol time line is depicted in Figure 1. The time points for perfusion imaging and angiogenesis imaging were selected on the basis of published results for peak angiogenesis and flow/perfusion restoration after vessel occlusion in the pig.²¹ We aimed to perform the final imaging and necropsy at 4 weeks (28 days) after initial studies but date varied by several days because of scheduling limitations. Pigs were injected via ear-vein catheter with 70.30 ± 10.0 MBq (1.90 ± 0.27 mCi) ^{201}Tl on day 1 and day 28 after FAO. The mean time between injection and imaging was 23.1 ± 13.7 minutes. Each pig was positioned supine on the palate of the scanner with the hind limbs extended. SPECT/CT imaging was performed on Philips Precedence camera (Philips, Andover, MA) using the following parameters: for the SPECT scan, ^{201}Tl window (30% window for 72 keV photopeak, 20% window for 168 keV photopeak), 60° circular orbit (180° per head) for 64 steps, 40 seconds/step. For the low-energy general all-purpose collimator, the spatial resolution at 10 cm ± 8 mm. Parameters for the spiral CT scan were the following: 120 KV, 3-mm slice thickness, 3-mm increments, and 25 mAs/slice.

Angiogenesis Imaging

On day 7 after vascular occlusion, pigs were sedated, intubated, and anesthetized, as described above.

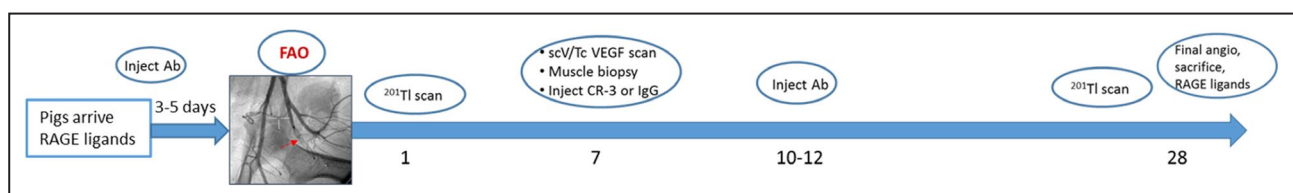


Figure 1. Protocol time line from arrival of pigs to final angiogram (angio) and euthanasia.

See text for justification of time points. The final procedures were planned to occur as close to 28 days (4 weeks) as possible. Ab indicates antibody; CR-3, anti-RAGE antibody; FAO, femoral artery occlusion; RAGE, receptor for advanced glycation end products; and VEGF, vascular endothelial growth factor.

^{99m}Tc -labeled scV was prepared as previously described.²² A dose of 303.4 ± 81.4 MBq (8.2 ± 2.2 mCi) of scV/Tc was injected through the ear vein catheter. The pigs remained anesthetized after injection to allow for blood pool clearance until transportation to imaging laboratory. The average time between tracer injection and imaging was $3:25 \pm 0:39$ hours. Pigs underwent SPECT/CT imaging on the Philips Precedence scanner using the following parameters: for the SPECT scan, ^{99m}Tc window (20% window for 140 KeV photopeak), 360° circular orbit (180° per head) for 64 steps, and 30 seconds/step. The CT parameters were the same as described above.

Muscle Biopsies

Approximately 2 hours after injection of scV/Tc, hind limb muscle biopsies were obtained. Hair was shaved over small segments of the semimembranosus, biceps femoris and gastrocnemius. An incision approximately 1 cm in length was made with a scalpel and subcutaneous tissue was gently pushed aside down to muscle surface, and using 4-mm diameter biopsies, 2 biopsies were taken from each site on both the ischemic hind limb and the opposite (control) hind limb. The wounds were closed with sutures and dressed. They healed well without signs of inflammation.

γ Counting

γ Well counting was performed to analyze hind limb muscle angiogenesis and tissue perfusion. Biopsy samples were weighed, counted in the γ well counter, fixed, embedded, and sectioned for histology.

Contrast Angiogram and Necropsy

On the day following the final ^{201}Tl scan, pigs underwent a contrast angiogram of the hind limb circulation. Following sedation, intubation, and under general anesthesia, using sterile conditions, a cut down was performed on the right carotid artery and catheters were advanced to the distal aorta just proximal to the iliac bifurcation. Iodinated contrast (678-mg Optiray 320) was selectively injected into each common FA, and images were obtained to include the anterior FA proximal and distal to the occluder and the profunda branch. Following this final angiogram, sedation was deepened and pigs were euthanized with euthanasia solution (Euthasol; 100 mg/kg IV) by veterinary staff. At necropsy, approximately 3 to 4 cm^3 muscle samples were taken from the proximal and distal gastrocnemius, biceps femoris, semimembranosus, and semitendinosus for both hind limbs. Two 1- cm^3 samples were taken from each of these larger sections, weighed, and counted on γ well counter. Using standards taken from

the injected dose, the γ counting data were converted to percentage injected dose per gram (%ID/g) of tissue. The remainder of the tissue was fixed, paraffin embedded, and sectioned for histology.

Scan Analysis

DICOM files, including the attenuation-corrected SPECT/CT images of hind limbs, were uploaded onto MIM 64-bit software (MIM Software, Cleveland, OH). Using the CT image, hind limb muscle groups, including the semimembranosus, semitendinosus, biceps femoris, and gastrocnemius, were identified. SPECT scans were carefully aligned and merged with the CT scans. Using operator-guided identification of fiducial points and computer-assisted boundary definition, 3-dimensional contours of each muscle were determined. Using the statistics function, total counts and volumes in cc were recorded for each muscle. Counts were converted to %ID with conversion factors derived from phantom experiments in which 1.0 mCi of either ^{201}Tl or ^{99m}Tc was placed in 1.0-cc Eppendorf tube suspended in middle of a phantom and scan acquired using same protocol as the pig scans.

To investigate effect of CR-3 on muscle viability, we compared volume (mass) of gastrocnemius muscle in the occluded limb at 4 weeks in the diabetic pigs treated with CR-3 versus diabetic pigs treated with nonimmune IgG.

Contrast Angiogram Analysis

Images were obtained from OEC digital fluoroscope model 7900 (General Electric, Chicago, IL) and uploaded onto a computer running ImageJ software. Segments of the anterior FA distal to the occluder and the profunda artery with similar backgrounds were selected, and a region of interest of the same size was placed over the 2 vessels. Using the measuring tool, mean value for contrast intensity was measured for the 2 vessels and ratios were determined for the occluded segment over the normal artery for both the nondiabetic and diabetic animals.

Histological Analysis

Biopsy muscle tissue samples taken on day 7 (peak time for angiogenesis in pig model) were stained for angiogenesis with lectin and VEGFA and for RAGE. Muscle tissue taken at necropsy was stained for RAGE and for Sirius red (fibrosis). All tissue samples from biopsies and necropsy were placed in formalin for 48 hours, followed by 70% alcohol, and then embedded. For immunohistochemical analyses, serial sections were deparaffinized in xylene, treated with 0.3% hydrogen peroxide for 20 minutes, and incubated

in protein-free block (Dako Inc, Carpinteria, CA) for 10 minutes to inhibit the nonspecific binding of primary antibody. All sections were stained with hematoxylin and eosin. For RAGE staining, muscle sections were incubated overnight with humanized anti-RAGE antibody (50 µg/mL) followed by incubating for 30 minutes with biotinylated secondary antibody (1:200). Lectin (*Lycopersicon esculentum* lectin) binds to glycoproteins on the basement membrane of endothelial cells in sprouting capillaries. Staining for capillary sprouting was performed using biotinylated Griffonia Bandeiraea Simplicifolia Isolectin I (1:50) (Vector Laboratories, Burlingame, CA) and treated for 30 minutes with VECTASTAIN ABC reagent (Vector Laboratories), followed by 3',3'-diaminobenzidine substrate kit for peroxidase (Vector Laboratories), and counterstaining with Gill hematoxylin solution. Staining for VEGFA was performed using anti-VEGFA antibody (1:200) (Abcam, Cambridge, MA). Morphometric and immunohistochemical analyses of the arterial segments were performed using a Nikon Eclipse 50i confocal microscope (Nikon, Tokyo, Japan) and Image-Pro Plus software (Media Cybernetics Inc, Silver Spring, MD). Muscle tissue was stained with Sirius red using Picro Sirius Red Staining Kit (Abcam).

Quantitative Immunohistochemistry

The number of capillaries staining brown for lectin were counted in 4 to 5 randomly selected fields in each section. These numbers were averaged and expressed as capillaries per 200× field. The same method was used for quantifying VEGFA staining capillaries. Quantification of RAGE staining and Sirius red staining was performed using color recognition software on Image-Pro Plus.

RAGE Ligand Measurements

RAGE ligand S100B was measured from frozen sera samples taken from each pig at baseline and at end of study using commercially available kits for porcine subjects (Porcine S100 Calcium Binding Protein B ELISA Kit) (My BioSource, San Diego, CA). Each sample was measured in triplicate using standards, and results are expressed as ng/mL.

Statistical Analysis

Data statistics for each group are expressed as mean±SD, followed by the range. Comparisons of means between 2 groups for all variables were made using 2-sample *t* tests. For data with small range of values (small SDs) in both groups, we used equal variance; and for data with large range of values (large SDs), we used unequal variance. To examine change over time, we took the difference in outcome

values between follow-up and baseline, before applying *t* tests to compare groups. For comparisons involving 3 groups, further post hoc adjustment for multiple comparisons was made using the Bonferroni correction, where the *P* value is compared with $0.05/3=0.017$.

RESULTS

Animals

The average age of the pigs on arrival was 8.9 ± 0.3 months. The average weight at the end of the study was 31.9 ± 4.1 kg for IgG group and 27.7 ± 5.2 kg for the CR-3 treated group ($P=0.14$). The averages for morning blood glucose level for the first week ranged from 264 to 500 mg/dL for the IgG treated pigs and from 316 to 453 mg/dL for the CR-3 treated pigs (P =not significant). The averages for morning blood glucose level for week 4 ranged from 298 to 413 mg/dL for the IgG treated pigs and from 291 to 406 mg/dL for the CR-3 treated pigs (not significant).

Intravascular Occlusion

The occluders were successfully deployed in the lumen of the anterior FA just distal to the takeoff of the circumflex branch in all pigs. No contrast was seen in the vessel distal to the occluder at the time of placement.

Perfusion in Occluded Limb

There was a trend for hind limb muscle perfusion in muscles supplied partially or completely by the anterior FA distal to the occlusion (biceps femoris, semitendinosus, and gastrocnemius) to remain unchanged or fall between days 1 and 28 in IgG treated pigs and to increase in CR-3 treated pigs (Figure 2A). The greatest uptake (perfusion) was to the gastrocnemius, which is the major muscle supplied by the anterior FA. Individual values for uptake of ^{201}Tl as %ID for the gastrocnemius muscles of pigs treated with CR-3 all increased with one exception, whereas individual values for IgG treated all fell (Figure 2B). The difference in the mean change in the gastrocnemius from day 1 to day 28 was significantly higher for the CR-3 treated pigs (0.2 ± 4 %ID) compared with the IgG treated (-0.18 ± 0.07 %ID) ($P=0.0024$) (Figure 2C).

FA Reconstitution

Contrast angiograms performed 4 weeks after placement of the occluder in the anterior FA from a representative pig treated with control IgG and one treated with CR-3 and an additional age- and weight-matched normal Yucatan minipig are shown in Figure 3. The normal pig shows good opacification (contrast density) of

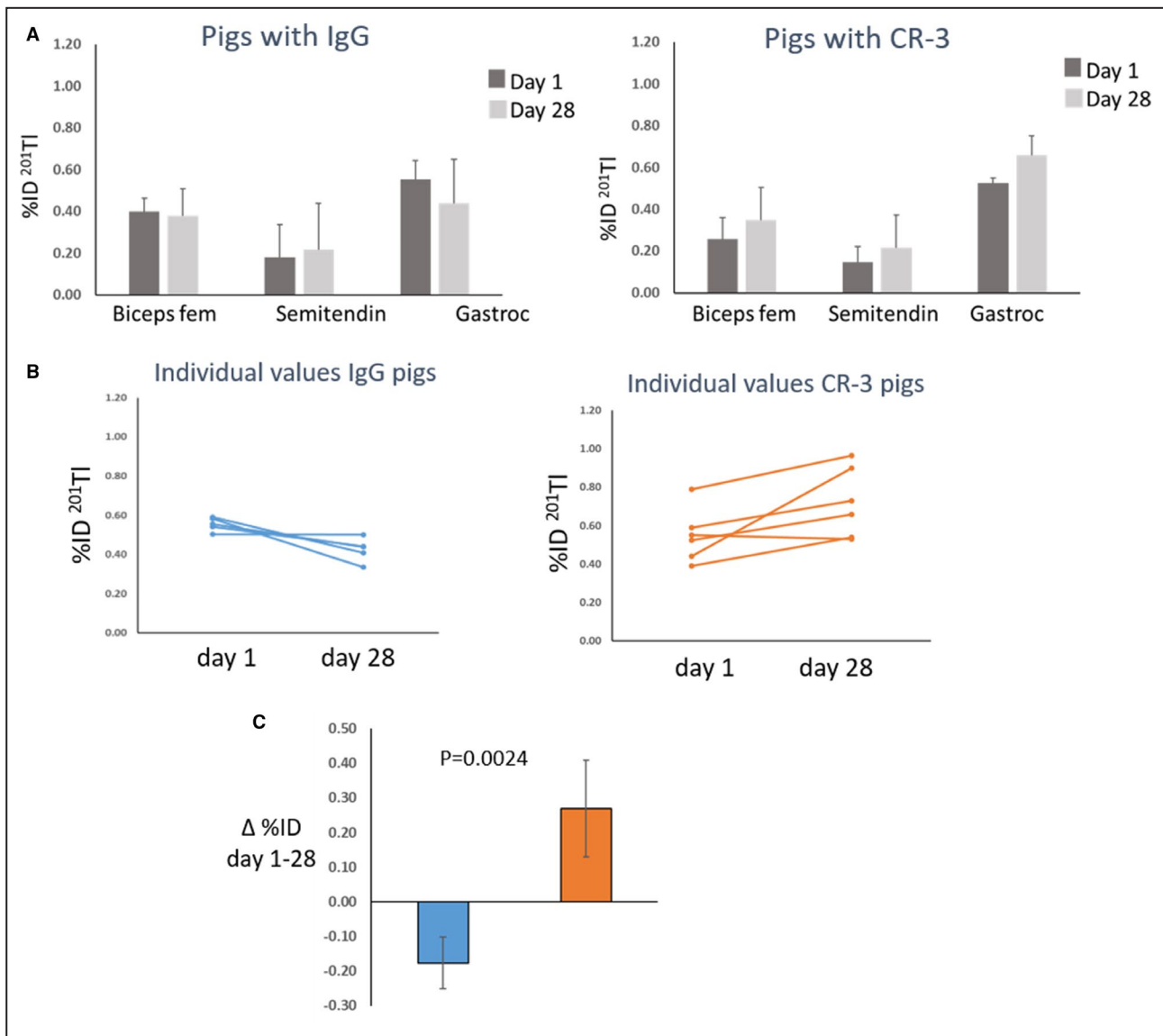


Figure 2. Effect of treatment on perfusion.

(A) Bars represent hind limb muscle perfusion measured as mean±SD uptake of ²⁰¹Tl (percentage injected dose [%ID]) for diabetic pigs treated with IgG (n=5) and anti-receptor for advanced glycation end products antibody (CR-3) (n=6) at day 1 (dark gray bars) and day 28 (light gray bars). (B) Individual values for gastrocnemius (Gastroc) muscle perfusion at day 1 and day 28 for IgG treated pigs (blue) and CR-3 treated pigs (orange). (C) Each bar represents change in Gastroc muscle perfusion as mean±SD between days 1 and 28 for IgG treated pigs (blue bar) and CR-3 treated pigs (orange bar). Biceps fem indicates biceps femoris; and Semitendin, semitendinosus.

the anterior FA immediately distal to the occluder and collaterals coming from the profunda and circumflex arteries. The diabetic pig treated with IgG shows poor to absent contrast density of the FA distal to the occluder and fewer collaterals than the normal pig. The pig treated with CR-3 shows good contrast density of the artery distal to the occluder and more collaterals from the circumflex branch than seen in the IgG treated pig. Ratios for contrast densities in the vessel distal to the occluder compared with the profunda artery were calculated for all pigs, and mean values for the 3 groups are shown in the bars in Figure 3. The mean value for the normal (nondiabetic pigs) was 0.94 ± 0.10 (range,

$0.86\text{--}1.09$); for the IgG treated pigs, 0.74 ± 0.10 (range, $0.56\text{--}0.82$); and for the CR-3 treated pig, 0.93 ± 0.12 (range, $0.82\text{--}1.12$) (Figure 3). *P* values for the IgG treated pigs versus the nondiabetic (normal) pigs (*P*=0.015) and for the IgG treated diabetic pigs versus the CR-3 treated pigs (*P*=0.012) were both statistically significant, applying the Bonferroni cutoff value.

Perfusion in Nonoccluded Limb Related to RAGE

To investigate effect of blocking RAGE on limb perfusion in diabetes mellitus independent of collaterals,

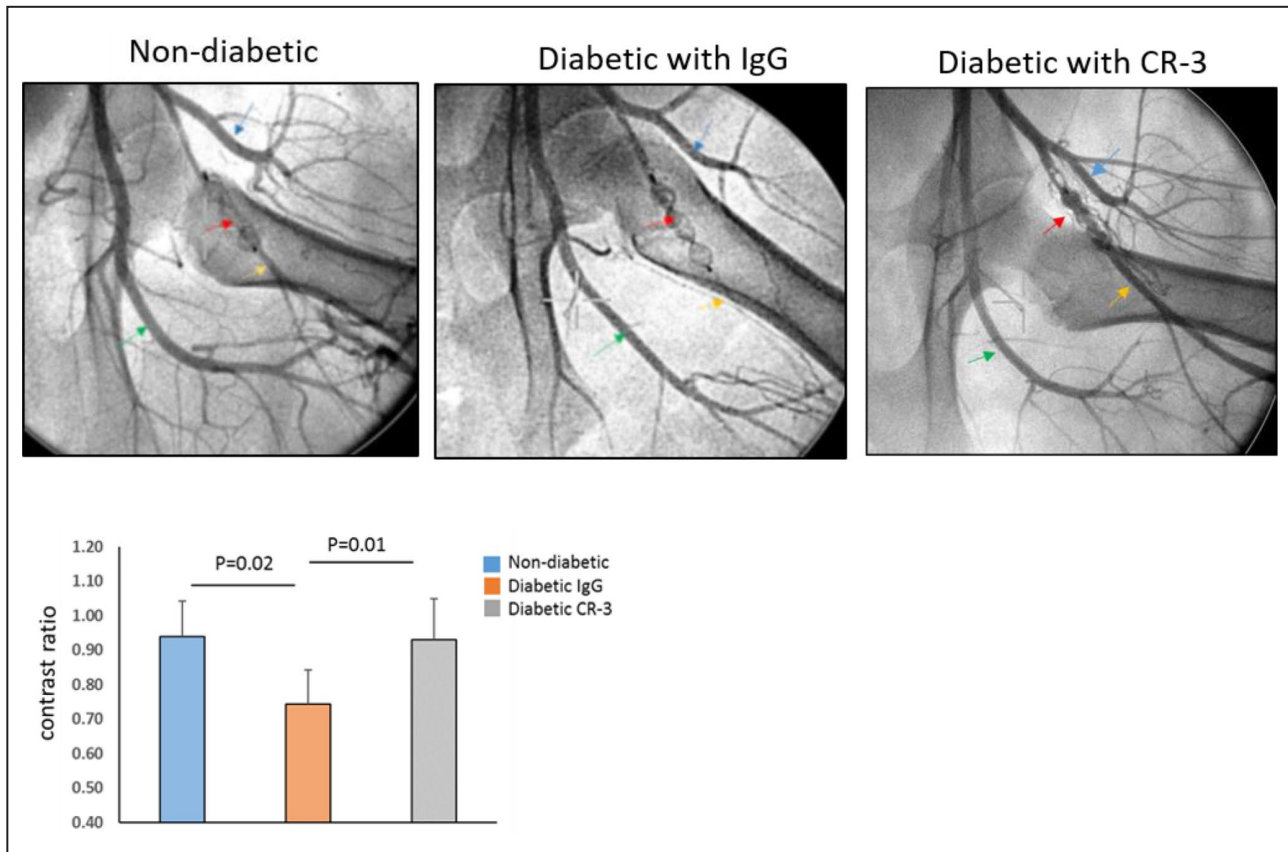


Figure 3. Collateral formation.

Contrast angiograms performed 4 weeks after femoral artery (FA) occlusion and 1 day before euthanasia. Red arrows point to the occluder, yellow arrows to anterior FA distal to the occluder, blue arrows to circumflex artery, and green arrows to profunda branch. The bar graph shows ratio of contrast intensities in the anterior FA distal to the occluder compared with the profunda. The legend identifies the bars. CR-3 indicates anti-receptor for advanced glycation end products antibody.

we measured change in ^{201}Tl uptake from initial to final scan in the gastrocnemius muscle of the nonoccluded hind limb in the 2 diabetic groups. There was variability in the individual responses among pigs but in general perfusion fell in the IgG treated pigs (-0.17 ± 0.26 %ID) (mean \pm SD) and rose in the CR-3 treated pigs (0.16 ± 0.16 %ID) ($P=0.03$ CR-3 versus IgG) (Figure 4A). Histological staining for RAGE from muscle samples showed positive staining for RAGE in the arterioles in the IgG treated pigs compared with minimal staining in similar size vessels in the normal pig and in the CR-3 treated pig (Figure 4B). Muscle samples were also counted in the γ well counter immediately following necropsy. The mean values for uptake of ^{201}Tl as %ID/g for the normal pigs was 3.00 ± 1.30 (range, 1.31–5.74); for the diabetic pigs treated with IgG, it was 2.03 ± 0.85 (range, 1.11–3.24); and for the CR-3 treated pigs, it was 3.15 ± 0.85 (range, 1.61–7.07) ($P=0.04$ versus IgG treated), supporting the scan data.

Angiogenesis

The pigs treated with CR-3 showed uptake of scV/Tc, indicating VEGF receptor expression in the proximal

gastrocnemius muscle, whereas the IgG treated pigs showed no uptake corresponding to location of this muscle on SPECT/CT scans (Figure 5A). The mean ratios of counts converted to %ID for the occluded to the nonoccluded limb were 1.35 ± 0.10 (range, 1.24–1.50) for the CR-3 treated pigs and 1.04 ± 0.13 (range, 0.90–1.21) for the diabetic pigs treated with IgG ($P=0.005$) (Figure 5B). γ Counting of muscle biopsies taken before the scans showed similar results. The average count ratio converted to %ID/g for the occluded to the nonoccluded limb was 1.30 ± 0.27 (range, 0.91–1.85) for the CR-3 treated pigs and 1.04 ± 0.20 (range, 0.72–1.25) for the IgG treated pigs ($P=0.026$).

Quantitative immunohistology supported the scan and tissue well counting data. More capillaries stained positive for lectin on tissue sections from muscle biopsies taken at day 7 after FAO (same samples used for γ well counting) for CR-3 treated pigs compared with IgG treated pigs (Figure 5C). The number of capillaries staining plus for lectin per field averaged over 4 fields/biopsy was 38.8 ± 7.1 (range, 33.3–48.0) for CR-3 treated and 19.0 ± 5.1 (range, 19.0 \pm 5.1) for the

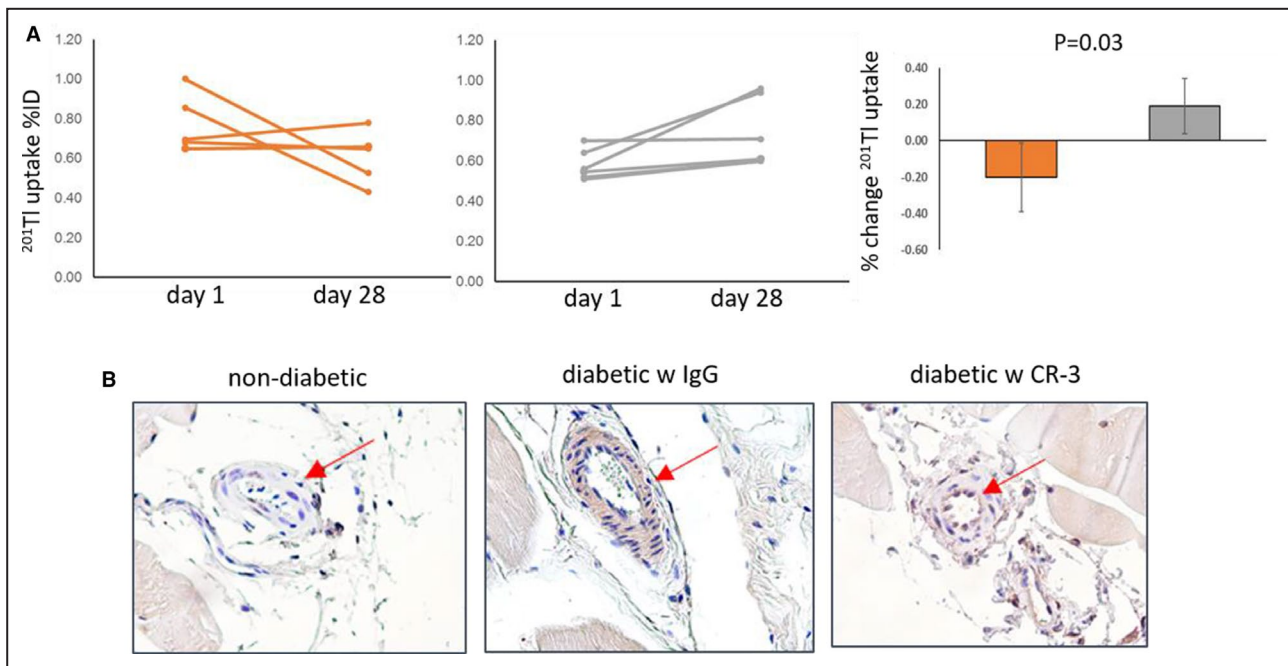


Figure 4. Gastrocnemius perfusion and receptor for advanced glycation end products (RAGE) staining.

(A) Individual responses in uptake of ^{201}Tl in gastrocnemius muscle from the nonischemic limb from baseline to final imaging for IgG treated (orange) and anti-RAGE antibody (CR-3) treated pigs (gray) and percentage change from baseline to final imaging. Orange bar, IgG treated; gray bar, CR-3 treated. (B) Immunostained sections of gastrocnemius muscle taken at necropsy from nondiabetic, IgG, and CR-3 treated diabetic pigs. Red arrows point to the red-brown staining for RAGE in arterioles. %ID indicates percentage injected dose.

IgG treated pigs ($P=0.004$) (Figure 5D). Staining for VEGFA showed greater staining in the CR-3 treated pigs compared with the IgG treated pigs (Figure 5E). Capillaries staining positive for VEGFA were higher in CR-3 treated pigs than IgG treated pigs (34 ± 10 versus 12 ± 1) ($P=0.009$) (Figure 5F).

Muscle Loss and Fibrosis

The change in mean gastrocnemius muscle volume from baseline to 4 weeks for the IgG treated pigs was -35 ± 19.4 cc; and for the CR-3 treated pigs, it was 10.2 ± 14.4 cc. The difference was statistically significant ($P=0.002$) (Figure 6A). Supporting the premise that the loss in volume was caused by loss of muscle tissue, the average percentage of sections staining positive for Sirius red (fibrosis) was greater in the IgG treated pigs (32.64 ± 8.9) compared with CR-3 treated pigs (14.24 ± 3.15), and the difference was statistically significant ($P=0.03$) (Figure 6B).

RAGE Ligands

Serum samples for S100B RAGE ligand were taken from diabetic pigs on arrival before treatment and before euthanasia. Figure 7 shows results for the final sample measurements for the IgG and CR-3 treated pigs. The mean value for the IgG treated pigs was 5.78 ± 2.62 (range, 3.75–10.88) ng/mL; and for the

CR-3 treated pigs, it was 2.86 ± 1.23 (range, 0.69–4.19) ng/mL. Applying a t -test with unequal variance, $P=0.025$. Plots showing the means and individual values for each group are shown in Figure 7A. Plots of values for individual pigs with evaluable samples for both initial and final time points are shown in Figure 7B.

Discussion

RAGE plays an important role in the cause and progression of PAD in diabetes mellitus through multiple pathways generating reactive oxygen species, increasing vascular permeability, releasing cytokines, and stimulating inflammation.^{10–16} In response to vascular occlusion, RAGE inhibits the hypoxic response to stimulate angiogenesis via hypoxia-inducible factor-1 α and VEGF expression.^{17–20} All of these factors contribute to the progression of PAD. We showed in this large animal model of diabetic PAD that blocking RAGE with a humanized anti-RAGE antibody improved hind limb perfusion both in the occluded limb, with greater reconstitution of the occluded vessel from collaterals, and improved perfusion to the nonoccluded limb independent of collaterals. Blocking RAGE also overcame the inhibition of the angiogenic response to tissue hypoxia and reduced muscle loss.

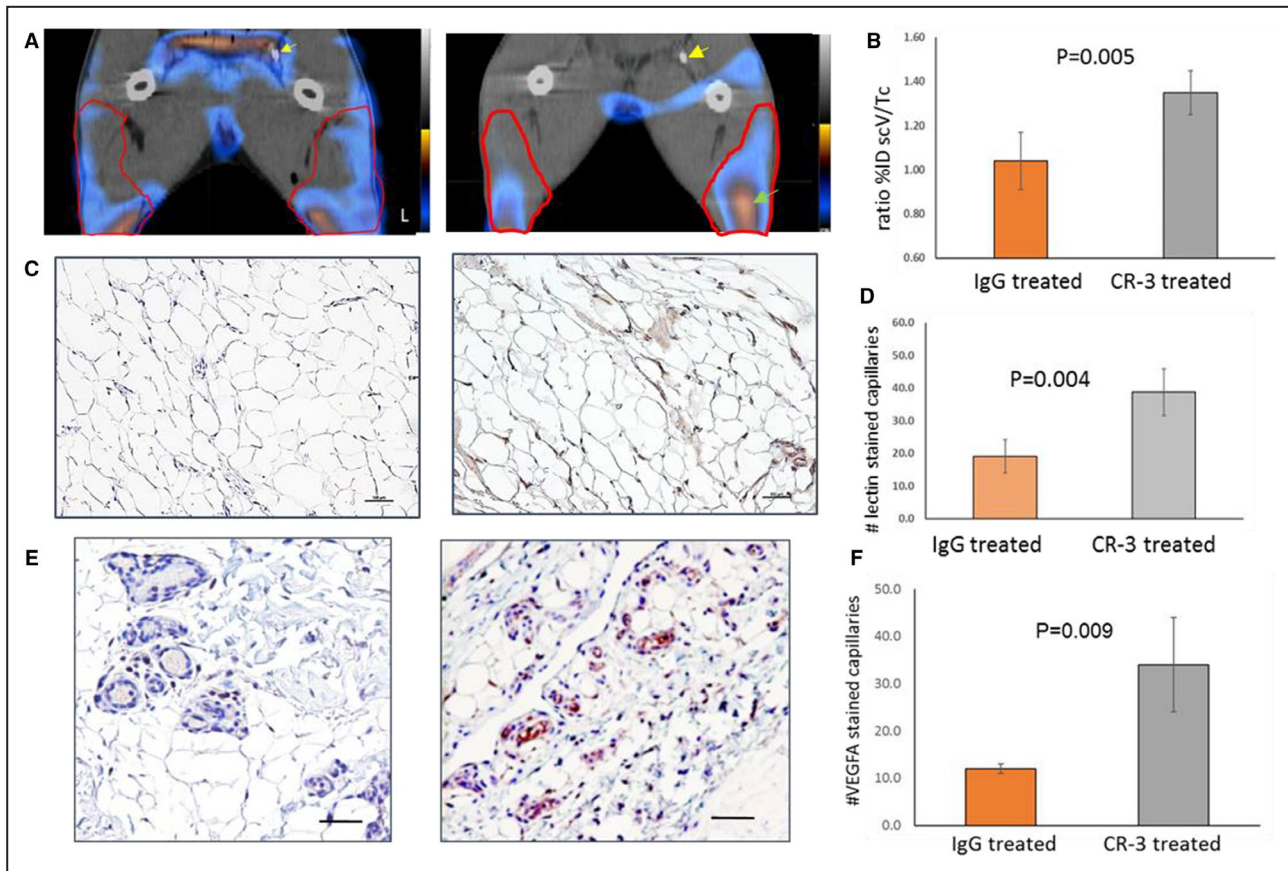


Figure 5. Angiogenesis imaging and capillary staining.

(A) Coronal single-photon emission computed tomography/x-ray computed tomography scV/Tc scans from a pig treated with IgG on left and pig treated with anti-receptor for advanced glycation end products antibody (CR-3) on the right. The yellow arrow points to the occluder. The red line outlines the gastrocnemius muscle. The green arrow points to the greater uptake of scV/Tc in gastrocnemius in the CR-3 treated pig compared with IgG treated pig. (B) Bars represent mean±SD for ratios of percentage injected dose (%ID) of uptake of scV/Tc for the IgG treated pigs (orange bar) and CR-3 treated pigs (gray bar). (C) Lectin staining for capillaries shows more abundant capillaries in CR-3 treated (right) compared with IgG (left). (D) Bars represent mean±SD quantitative lectin staining. (E) Immunostaining for vascular endothelial growth factor A (VEGFA) showing greater capillary staining in muscle from CR-3 treated pigs. (F) Bars represent mean±SD for quantitative VEGFA staining.

Our anti-RAGE antibody binds a unique peptide sequence on the V domain of the receptor. In the antibody development, we first developed a murine antibody with hybridoma technology by immunizing mice to the unique peptide and producing IgG2a isotype with κ light chain antibodies.²³ Subsequently, we humanized the anti-RAGE antibody using the chimeric antibody intermediary process. The antibody cDNA was cloned and expressed on mammalian cells and then large-scale antibody produced using plasmid technology (AvantGen, San Diego, CA). The humanized anti-RAGE antibody (CR-3) is IgG1 isotype. We showed blocking properties for the murine antibody²⁰ and repeated results with the humanized antibody in cell culture experiments.

The RAGE receptor is a multiligand receptor and binds specific ligands that are elevated in different disease and organ-specific conditions. Among these ligands are advanced glycation end products,

high-mobility group box 1, and the S100 calgranulins.²⁴ In patients with PAD, higher plasma levels of the ligand S100 calgranulin A12 were associated with shorter amputation-free survival in diabetic patients.²⁵ In the pigs in our study, we found higher values for S100 calgranulin B in diabetic pigs treated with IgG compared with pigs treated with CR-3. For individual pigs with available samples taken before and after treatment, ligand values fell for the CR-3 treated pigs compared with unchanged values for the IgG treated pigs. Although the samples sizes are small, these data suggest that by blocking the binding of the ligand to the receptor, CR-3 broke the positive receptor/ligand feedback loop, thereby reducing circulating ligand levels.

We and others have shown beneficial effects of reducing RAGE expression to restore angiogenesis and limb perfusion in murine models of hind limb ischemia induced by FAL.^{17,21,26,27} Approaches include

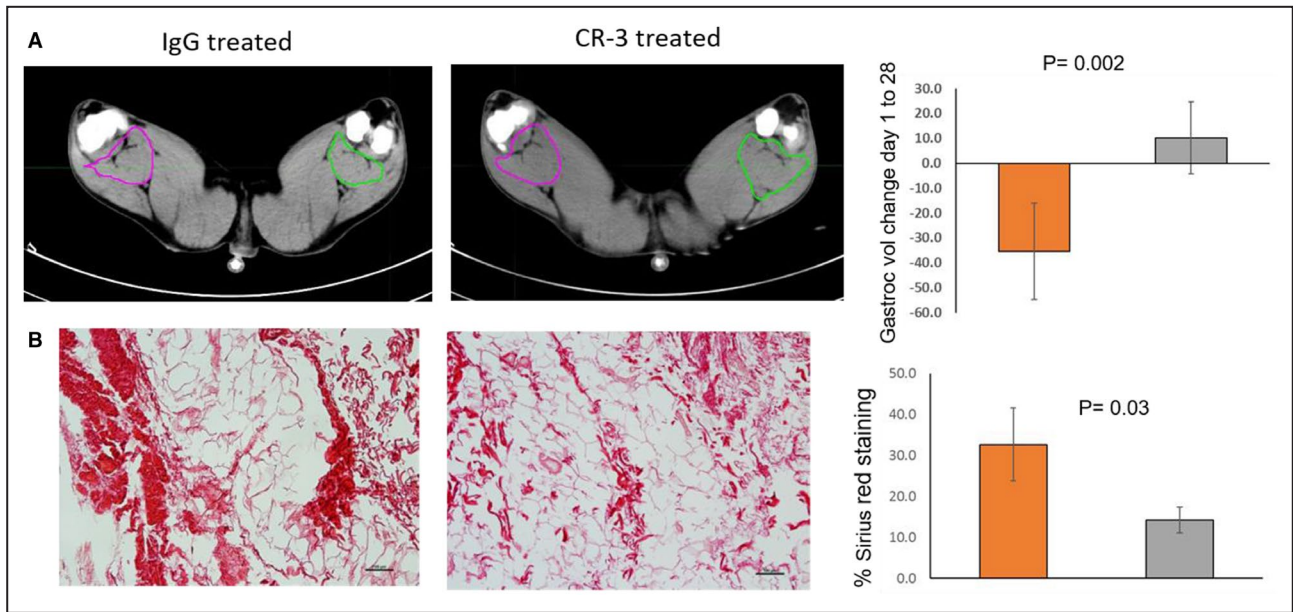


Figure 6. Muscle volume and fibrosis.

(A) Transverse x-ray computed tomography scans from final study (4 weeks) with color outlines showing margins of gastrocnemius (Gastroc) muscle showing smaller area on side of occluder (green) compared with opposite in IgG treated, whereas the areas are similar in anti-receptor for advanced glycation end products antibody (CR-3) treated pig. Muscle volumes decreased during study in IgG treated compared with CR-3, shown in bars on right. (B) Histological staining with Sirius red for fibrosis, showing greater staining in IgG treated compared with CR-3, as shown in bars on right. Values represent mean±SD. Orange bar, IgG treated; gray bar, CR-3 treated. Vol indicates volume.

blocking antibodies and inducing or injecting decoys. Endosecretory RAGE or soluble RAGE act as decoys and bind circulating ligands, thereby reducing ligand/receptor binding. Diabetic mice treated with soluble RAGE and transgenic diabetic mice overexpressing endosecretory RAGE showed greater angiogenesis in the ischemic hind limb compared with untreated diabetic mice with FAL.^{17,27} We showed the effect of eliminating RAGE on restoring the angiogenic response to FAL in nondiabetic and diabetic RAGE+/+ and RAGE-/- mice with micro-SPECT/CT imaging of radiolabeled RGDs targeting αvβ3 integrin expression.²⁸

Interruption of blood flow acutely cuts the supply of oxygen and nutrients to tissue, resulting in tissue loss, and over time, replacement by fibrosis.²⁹⁻³¹ A major effect of angiogenesis is to improve local tissue perfusion, delivering oxygen and nutrients and thereby salvaging hypoxic tissue. In the diabetic pigs treated with CR-3, we showed the beneficial effect of restoring the angiogenic response to improve tissue viability manifest as a reduction in muscle volume loss and lower muscle fibrosis after 4 weeks of treatment.

Both angiogenesis and arteriogenesis help reestablish flow distal to an occluded artery.³²⁻³⁵ The 2

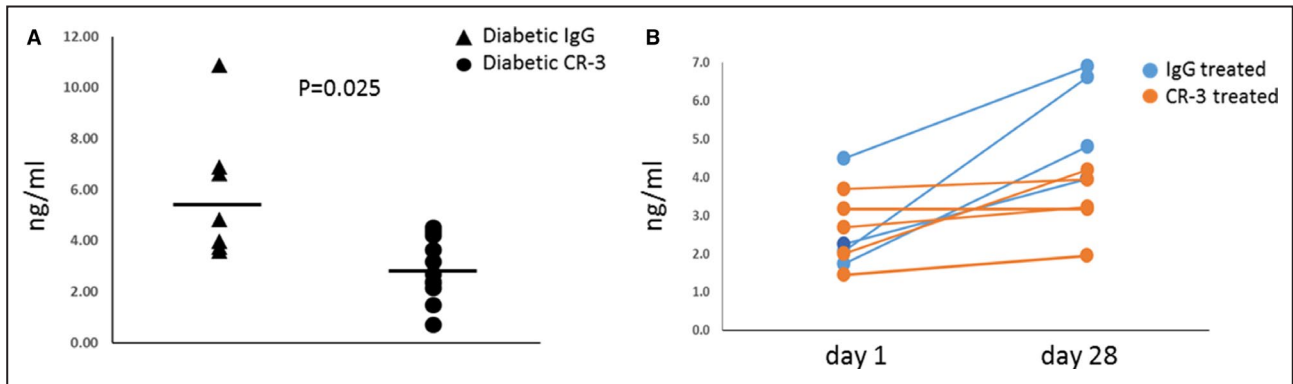


Figure 7. Receptor for advanced glycation end products (RAGE) ligands.

(A) Scatter graph shows values for serum levels of S100B calgranulins in ng/mL in the 2 groups of pigs identified in the legend. The significance levels between groups are displayed in graph. (B) Shows values for S100B measured from sera taken at day 1 and day 28 for individual pigs treated with IgG (blue) and anti-RAGE antibody (CR-3) (orange).

processes have different mechanisms. As described above, angiogenesis is a dynamic process at the molecular level initiated by hypoxic stimulus. For the capillary networks to grow, the extracellular matrix is remodeled for the proliferating endothelial cells, forming microvessels. The formation of collaterals in response to vessel occlusion involves physical stimuli that create increased shear stress to preexisting collateral vessels.³³ This physical force stimulates expression of adhesion molecules, cytokines, and growth factors by the endothelium, leading to outward remodeling of the vessel wall to form a larger artery.³³ Patients with diabetes mellitus show poor collateral formation in response to vascular stenosis or occlusion. On the basis of greater contrast density in the anterior FA distal to the occlusion and more collaterals assessed visually at the site of arterial occlusion with CR-3 treatment suggests that RAGE plays a role in suppressing collateral formation. The mechanism whereby RAGE suppresses this process is unknown, but we could speculate that diffuse vascular disease of diabetes mellitus involving the preexisting collateral vessels blocks the molecular pathways stimulated by shear stress.

Diabetic PAD is typically diffuse, involving proximal and distal vessels. RAGE is expressed in the arterial walls of patients with PAD.³⁶ At the microvascular level, RAGE expression impairs vasoreactivity.¹⁵ Although we did not test for vasoreactivity or measure peripheral resistance in our study, we did find reduced perfusion in the distal gastrocnemius in the nonoccluded hind limb of the IgG treated diabetic pigs compared with normal pigs, which corresponded to increased RAGE staining in arterioles. The CR-3 treated diabetic pigs showed higher perfusion than the IgG treated pigs and less RAGE staining in the arterioles.

Limitations

Although the pigs we used in this study are a better model of type 1 diabetes mellitus than type 2, there are several reasons to select this model. The purpose-bred diabetic Yucatan minipigs have blood glucose levels in the range of patients with PAD, and the level of blood sugar is shown to be the most important association with PAD in clinical studies.² Limb ischemia in patients results from atherosclerotic occlusion. Purpose-bred diabetic pigs have minimal atherosclerotic lesions and therefore we performed intra-arterial occlusion of a major artery in one hind limb, to produce limb ischemia. Our model is different from the pig models of peripheral arterial occlusion previously reported. Both Stacy et al²¹ and Gao et al³⁵ performed surgical ligation in nondiabetic Yorkshire pigs. These models present limitations in

assessing angiogenesis separate from wound healing response to surgical intervention. Long et al³⁷ performed endovascular occlusion in the external iliac in nondiabetic Yorkshire pigs. This model leads to extensive ischemia in the hind limb and is better applicable for studying muscle damage.

We gave first dose of antibody several days before FAO. The timing of onset of treatment in relationship to injury requires further experiments.

CONCLUSIONS

High RAGE expression in diabetes mellitus is implicated in many of the diabetic vascular complications, including PAD. We have shown in a large animal model of diabetes mellitus and hind limb arterial occlusion that treatment with a RAGE-blocking antibody improves hind limb muscle perfusion, angiogenesis, and collateral growth in response to arterial occlusion and improves perfusion to the nonoccluded limb, corresponding to reduced vessel staining for RAGE. Our model does not emulate all features of human PAD and therefore our results must be interpreted with caution. However, combined with our similar data from diabetic mouse FAL experiments, these results in 2 species suggest this antibody shows promise for a clinical treatment for diabetic PAD.

ARTICLE INFORMATION

Received March 20, 2020; accepted October 19, 2020.

Affiliations

From the Department of Medicine, Columbia University Medical Center, New York, NY (L.L.J., J.J., R.O., A.H., G.Z., Z.A., Y.T.); and SibTech, Inc, Brookfield, CT (M.B., J.B.).

Sources of Funding

This work was supported by National Heart, Lung, and Blood Institute R01 HL130056 to Dr Johnson (principal investigator). Abbott Laboratories provided us with a grant to provide 20 Amplatzer Vascular Plug II, 8 mm (9-AVP2-008).

Disclosures

None.

REFERENCES

1. Fowkes FGR, Aboyans V, Freya J, Fowkes I, McDermott MM, Sampson UK, Criqui MH. Peripheral artery disease: epidemiology and global perspectives. *Nat Rev Cardiol*. 2017;14:156–170.
2. Selvin E, Marinopoulos S, Berkenblit G, Rami T, Brancati FL, Powe NR, Golden SH. Meta-analysis: glycosylated hemoglobin and cardiovascular disease in diabetes mellitus. *Ann Intern Med*. 2004;14:421–431.
3. Anand SS, Caron F, Eikelboom JW, Bosch J, Dyal L, Aboyans V, Abola MT, Branch KRH, Keltai K, Bhatt DL, et al. Major adverse limb events and mortality in patients with peripheral artery disease: the COMPASS Trial. *J Am Coll Cardiol*. 2018;71:2306–2315.
4. Low Wang CC, Blomster JL, Heizer G, Berger JS, Baumgartner I, Fowkes FGR, Held P, Katona BG, Norgren L, Jones WS, et al. Cardiovascular and limb outcomes in patients with diabetes and peripheral artery disease: the EUCLID Trial. *J Am Coll Cardiol*. 2018;72:3274–3284.

5. Brownrigg JRW, Schaper NC, Hinchliffe RJ. Diagnosis and assessment of peripheral arterial disease in the diabetic foot. *Diabet Med*. 2015;3:738–747.
6. Gerhard-Herman MD, Gornik HL, Barrett C, Barshes NR, Corriere MA, Drachman DE, Fleisher LA, Fowkes FGR, Hamburg NM, Kinlay S, et al. 2016 AHA/ACC guideline on the management of patients with lower extremity peripheral artery disease. *Circulation*. 2017;135:e686–e725.
7. Perez P, Esteban C, Sauquillo JC, Yeste M, Manzano L, Mujal A, Caballero PEJ, Aguilar E, Munoz-Torrero JFS, Monreal M. Cilostazol and outcome in outpatients with peripheral artery disease. *Thromb Res*. 2014;134:331–335.
8. Shishehbor MH, Jaff MR. Percutaneous therapies for peripheral artery disease. *Circulation*. 2016;134:2008–2027.
9. Schmidt AM, Yan SD, Wautier JL, Stern DM. Activation of receptor for advanced glycation end products: a mechanism for chronic vascular dysfunction in diabetic vasculopathy and atherosclerosis. *Circ Res*. 1999;84:489–497.
10. Kalea A, Schmidt AM, Hudson B. RAGE: a novel biological and genetic marker for vascular disease. *Clin Sci (Lond)*. 2009;116:621–637.
11. Wendt T, Bucciarelli L, Qu W, Lu Y, Yan SF, Stern DM, Schmidt AM. Receptor for advanced glycation endproducts (RAGE) and vascular inflammation: insights into the pathogenesis of macrovascular complications in diabetes. *Curr Atherosclerosis Rep*. 2002;4:228–237.
12. Wautier JL, Wautier MP, Schmidt AM, Anderson GM, Hori O, Zoukourian C, Capron L, Chappey O, Yan SD, Brett J, et al. Advanced glycation endproducts (AGEs) on the surface of diabetic erythrocytes bind the vessel wall via a specific receptor inducing oxidant stress in the vasculature: a link between surface-associated AGEs and diabetic complications. *Proc Natl Acad Sci*. 1994;91:7742–7746.
13. Nawroth PP, Stern DM. Soluble forms of RAGE: an index of vascular stress? A commentary on soluble RAGE in type 2 diabetes: association with oxidative stress. *Free Radical Bio Med*. 2007;43:506–510.
14. Bassirat M, Khalil Z. Short-and long-term modulation of microvascular responses in streptozotocin-induced diabetic rats by glycosylated products. *J Diabetes Complications*. 2010;24:64–72.
15. Yao D, Brownlee M. Hyperglycemia-induced reactive oxygen species increase expression of the receptor for advanced glycation end products (RAGE) and RAGE ligands. *Diabetes*. 2010;59:249–255.
16. Waltenberger J. VEGF resistance as a molecular basis to explain the angiogenesis paradox in diabetes mellitus. *Biochem Soc Trans*. 2009;37:1167–1170.
17. Shoji T, Koyama H, Moriako T, Tanaka S, Kizu A, Montoyama K, Mori K, Fukumoto S, Shioi A, Shimogaito N, et al. Receptor for advanced glycation end products is involved in impaired angiogenic response in diabetes. *Diabetes*. 2006;55:2245–2255.
18. Hansen LM, Gupta D, Joseph G, Weiss D, Taylor WR. The receptor for advanced glycation end products impairs collateral formation in both diabetic and non-diabetic mice. *Lab Invest*. 2017;97:34–42.
19. Tchaikovski V, Olieslagers S, Böhmer FD, Waltenberger J. Diabetes mellitus activates signal transduction pathways resulting in vascular endothelial growth factor resistance of human monocytes. *Circulation*. 2009;120:150–159.
20. Tekabe Y, Anthony T, Li Q, Ray R, Rai V, Zhang G, Schmidt AM, Johnson LL. Treatment effect with anti-RAGE F(ab')₂ antibody improves hind limb angiogenesis and blood flow in type 1 diabetic mice with left femoral artery ligation. *Vasc Med*. 2015;20:212–218.
21. Stacy M, Yu D-Y, Maxfield M, Jaba IM, Jozwik BP, Zhuang ZW, Lin BA, Hawley CL, Caracciolo CM, Pal P, et al. Multimodality imaging approach for serial assessment of regional changes in lower extremity arteriogenesis and tissue perfusion in a porcine model of peripheral arterial disease. *Circ Cardiovasc Imaging*. 2014;7:92–99.
22. Tekabe Y, Kollaros M, Zerihoun A, Zhang G, Backer MV, Backer JM. Imaging VEGF receptor expression to identify accelerated atherosclerosis. *EJNMMI Res*. 2014;4:41–50.
23. Tekabe Y, Li Q, Rosario R, Sedlar M, Majewski S, Hudson BI, Einstein AJ, Schmidt AM, Johnson LL. Development of receptor for advanced glycation end products-directed imaging of atherosclerotic plaque in a murine model of spontaneous atherosclerosis. *Circ Cardiovascular Imaging*. 2008;1:212–219.
24. Bongarzone S, Savickas V, Luzi F, Gee A. Targeting the receptor for advanced glycation endproducts (RAGE): a medicinal chemistry perspective. *J Med Chem*. 2017;60:7213–7232.
25. Malmstedt J, Kärvestedt L, Swedenborg J, Brismar K. The receptor for advanced glycation end products and risk of peripheral artery disease, amputation or death in type 2 diabetes: a population-based cohort study. *Cardiovasc Diabetol*. 2015;14:93–102.
26. Tamarat R, Silvestre JS, Huijberts M, Benessiano J, Ebrahimiyan TG, Duriez M, Wautier M-P, Wautier JL, Levy BI. Blockade of advanced glycation end-product formation restores ischemia-induced angiogenesis in diabetic mice. *Proc Natl Acad Sci USA*. 2003;100:8555–8560.
27. Kim BH, Ko Y-G, Kim SH, Kim SH, Chung JH, Hwang K-C, Choi D, Jang Y. Suppression of receptor for advanced glycation end products improves angiogenic responses to ischemia in diabetic mouse hindlimb ischemia model. *ISRN Vasc Med*. 2013;8:1–8.
28. Tekabe Y, Shen X, Luma J, Weisenberger D, Yan SF, Haubner R, Schmidt AM, Johnson L. Imaging effect of receptor for advanced glycation endproducts on angiogenic response to hindlimb ischemia in diabetes. *EJNMMI Res*. 2011;1:3–12.
29. Ha DM, Carpenter LC, Koutakis P, Swanson SA, Zhu Z, Hanna M, DeSpiegelaere HK, Pipinos II, Casale GP. Transforming growth factor-beta 1 produced by vascular smooth muscle cells predicts fibrosis in the gastrocnemius of patients with peripheral artery disease. *J Transl Med*. 2016;14:39–53.
30. Lin Y-C, Chuang W-Y, Wei F-C, Yeh C-H, Tinhofer I, Deek NFA, Fu T-C, Ng S-C, Cahng T-C, Cheung Y-C. Peripheral arterial disease: the role of extracellular volume measurements in lower limb muscles with MRI. *Eur Radiol*. 2020;30:3943–3950.
31. Moyer AL, Wagner KR. Regeneration versus fibrosis in skeletal muscle. *Curr Opin Rheumatol*. 2011;23:568–573.
32. Kapanadze T, Bankstahl JP, Wittneben A, Koestner W, Ballmaier M, Gamrekelashvili J, Krishnasammy K, Limbourg A, Ross TL, Meyer G-J. Multimodality and multiscale analysis reveals distinct vascular, metabolic, and inflammatory components of tissue response to limb ischemia. *Theranostics*. 2019;9:152–166.
33. Hendriks G, Vöö S, Bauwens M, Post MJ, Mottaghy FM. SPECT and PET imaging of angiogenesis and arteriogenesis in pre-clinical models of myocardial ischemia and peripheral vascular disease. *Eur J Nucl Med Mol Imaging*. 2016;43:2433–2447.
34. Scholz D, Ziegelhoeffer T, Helisch A, Wagner S, Friedrich C, Podzuweit T, Schaper W. Contribution of arteriogenesis and angiogenesis to postocclusive hindlimb perfusion in mice. *J Mol Cell Cardiol*. 2002;34:775–787.
35. Ritthaler U, Deng Y, Zhang Y, Greten J, Mi A, Sido B, Allenberg J, Otto G, Roth H, Bierhaus A, et al. Expression of receptors for advanced glycation end products in peripheral occlusive vascular disease. *Am J Pathol*. 1995;3:688–694.
36. Gao Y, Aravind S, Patel NS, Fuglestad MA, Ungar JS, Mietus CJ, Li S, Casale GP, Pipinos II, Carlson MA. Collateral development and arteriogenesis in hindlimbs of swine after ligation of arterial inflow. *J Surg Res*. 2020;249:168–179.
37. Long CA, Timmins LH, Koutakis P, Goodchild TT, Lefer DJ, Pipinos II, Casale GP, Brewster LP. An endovascular model of ischemic myopathy from peripheral arterial disease. *J Vasc Surg*. 2017;66:891–901.